Acta Crystallographica Section F
Structural Biology and Crystallization Communications
ISSN 1744-3091

Crystallization and preliminary X-ray crystallographic analysis of human peptidylarginine deiminase type III

Masaki Unno,[a,b,c]* Kenji Kizawa,[d] Makiko Ishihara[a] and Hidenari Takahara[a,e]

[a]Frontier Research Center for Applied Atomic Sciences, Ibaraki University, 162-1 Shirakata, Tokai, Naka, Ibaraki 319-1106, Japan, [b]Graduate School of Science and Engineering, Ibaraki University, 2-1-1 Bunkyo, Mito, Ibaraki 310-8512, Japan, [c]Institute for Protein Research, Osaka University, 3-2 Yamadaoka, Suita, Osaka 565-0871, Japan, [d]Innovative Beauty Science Laboratory, Kanebo Cosmetics Inc., 5-3-28 Kotobuki, Odawara, Kanagawa 250-0002, Japan, and [e]Department of Applied Biological Resource Sciences, Ibaraki University, 3-21-1 Chuo, Ami, Inashiki, Ibaraki 300-0393, Japan

Correspondence e-mail: unno19@mx.ibaraki.ac.jp

Received 8 March 2012
Accepted 7 April 2012

In the presence of calcium ions, human peptidylarginine deiminase (PAD) converts arginine residues in proteins to citrulline. Of the five known human PAD enzymes, the type III isozyme (PAD3) exhibits the highest specificity for synthetic and natural substrates. This study aimed to determine the structure of PAD3 in order to elucidate its selective citrullination mechanism. Crystals of PAD3 obtained using polyethylene glycol 400 as a precipitant diffracted to 2.95 Å resolution using synchrotron radiation. They belonged to space group $R3$, with unit-cell parameters $a = b = 114.97$, $c = 332.49$ Å (hexagonal axes). Assuming two molecules were contained in an asymmetric unit, the calculated Matthews coefficient was 2.83 Å^3 Da^{-1}, corresponding to a solvent content of 56.6%. Initial phases were determined using PAD4 as a molecular-replacement model.

1. Introduction

Peptidylarginine deiminase (PAD; EC 3.5.3.15) is an enzyme that, in the presence of calcium ions, converts arginine residues in the target protein into citrullines (Vossenaar *et al.*, 2003). Protein citrullination by PAD confers large structural and mechanical effects on the target proteins by altering intermolecular and intramolecular ionic or hydrophobic interactions. In most cases, loss of the positive charge of the peptidylarginine residues disrupts intermolecular or intramolecular ionic interactions (Ying *et al.*, 2009).

Five paralogous genes (*PADI*1–4 and 6) on human chromosome 1p35-36 encode the human PAD isozymes (Chavanas *et al.*, 2004). PAD2 is distributed in ubiquitous tissues. PAD1 and PAD3 are specifically expressed in the epidermis and hair follicles (Kanno *et al.*, 2000; Nachat *et al.*, 2005), whereas PAD4 and PAD6 are absent from these epidermal tissues. In many cases, multiple PAD isotypes are responsible for introducing peptidylcitrulline residues into a target protein. The citrullination of epithelial substrates appears to be conducted by a set of PAD isozymes with narrow (*e.g.* PAD3) or broad (*e.g.* PAD1 or PAD2) substrate specificity. For example, filaggrin is modified by PAD1 and PAD3 in the skin epidermis (Méchin *et al.*, 2005), whereas S100A3 is modified by PAD2 and PAD3 in hair follicles (Kizawa *et al.*, 2008).

Among the PADs, PAD3 shows the highest substrate specificity for synthetic (Méchin *et al.*, 2005) and natural (Kizawa *et al.*, 2008) substrates. S100A3 is an EF-hand-type Ca^{2+}-binding S100 protein family member that colocalizes with PAD3 in hair cuticular cells (Kizawa *et al.*, 2011). PAD3 converts a symmetric pair of Arg51 residues on an S100A3 dimer surface to citrullines, causing assembly of a homotetramer, but does not convert other arginines (Kizawa *et al.*, 2008). Although this specific citrullination is largely affected by the formation of two intramolecular disulfides in S100A3, it is unclear how the sheltered Arg51 residue is recognized by PAD3 (Unno *et al.*, 2011).

Although X-ray crystal structures of the PAD4 isozyme and its complexes with substrate peptides have been reported (Arita *et al.*, 2003, 2004, 2006), structural analysis of other PAD isozymes has not yet been conducted. To elucidate how the citrullination mechanism(s) of PAD isozymes confer different substrate specificities, it is necessary to determine the X-ray structure of PAD3. In the present study,

we report the crystallization and preliminary X-ray crystallographic analysis of PAD3.

2. Experimental

2.1. Expression and purification

The recombinant vector for 6×His-tagged human PAD3 (pET16b-PAD3) was a kind gift from Professor P. R. Thompson (University of South Carolina). Expression of the His-tagged PAD3 protein in *Escherichia coli* BL21 (DE3) cells and purification using a chelating His-tag affinity column were conducted as reported previously (Knuckley *et al.*, 2010) with slight modifications. Briefly, cells cultured in 2 l LB medium were disrupted by sonication in 20 m*M* Tris–HCl buffer pH 7.6 containing 400 m*M* NaCl, 5 m*M* imidazole, 1% Triton X-100 and 10 m*M* β-mercaptoethanol (buffer *A*) supplemented with 1 m*M* phenylmethanesulfonylfluoride at 277 K. After centrifugation at 40 000*g* for 20 min, the supernatant was applied onto a HiTrap Chelating HP column (5 ml, GE Healthcare) which had been equilibrated with buffer *A*. The adsorbed fraction was eluted by increasing the imidazole concentration to 500 m*M*. Eluted fractions were collected and dialysed against 20 m*M* Tris–HCl buffer pH 7.6 containing 150 m*M* KCl, 2 m*M* dithiothreitol (DTT), 0.1 m*M* ethylenediaminetetraacetic acid (EDTA) and 10% glycerol (buffer *B*). The resulting sample was applied onto a HiTrap Q HP anion-exchange column (5 ml, GE Healthcare) which had been equilibrated with buffer *B*. The adsorbed fraction was eluted using buffer *B* with the KCl concentration increased to 1 *M*. Eluted fractions were further purified on a HiPrep 16/60 Sephacryl S-200 HR gel-filtration column (GE Healthcare) using buffer *B*. The homogeneity of the purified protein was confirmed by SDS–PAGE.

2.2. Crystallization

Purified protein in buffer *B* was concentrated to 2–8 mg ml^{-1} using an Amicon Ultra centrifugal filter (Millipore) at 277 K. Crystallization was performed by the hanging-drop vapour-diffusion method in a 24-well tissue-culture plate (Falcon). At first, crystallization of PAD3 was performed under similar conditions to those previously used for PAD4 (Arita *et al.*, 2003). Crystals were obtained at 293 K in hanging drops composed of 2 µl PAD3 solution in buffer *B* and 2 µl precipitant solution consisting of 20 m*M* imidazole buffer pH 7.0, 0.2 *M* Li_2SO_4, 15%(*w*/*v*) polyethylene glycol (PEG) monomethylether 5000. The best crystals were obtained with an optimized precipitant solution consisting of 0.1 *M* 4-(2-hydroxyethyl)-1-piperazineethanesulfonic acid (HEPES) buffer pH 7.5, 0.2 *M* NaCl, 25%(*v*/*v*) PEG 400. Fig. 1 shows a picture of the crystal.

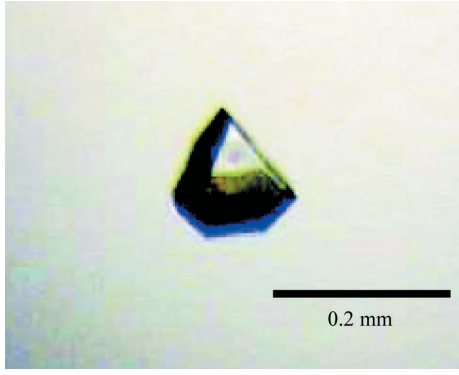

Figure 1
A hexagonal pyramid-shaped crystal of PAD3 obtained using PEG 400 as a precipitant.

Table 1
Data-collection statistics.

Values in parentheses are for the highest resolution shell.

X-ray source	SPring-8 BL44XU
Wavelength (Å)	0.9
Space group	*R*3
Unit-cell parameters	
$a = b$ (Å)	114.97
c (Å)	332.49
$\alpha = \beta$ (°)	90
γ (°)	120
Resolution range (Å)	50.0–2.95 (3.00–2.95)
$R_{\rm merge}$† (%)	8.7 (43.7)
Average $I/\sigma(I)$	28.89 (3.44)
No. of observations	334364
No. of unique reflections	34043
Data completeness (%)	99.9 (100.0)
Multiplicity	9.8 (9.8)
Crystal mosaicity (°)	0.83

† $R_{\rm merge} = \sum_{hkl}\sum_i |I_i(hkl) - \langle I(hkl)\rangle| / \sum_{hkl}\sum_i I_i(hkl)$, where $I_i(hkl)$ is the intensity of the ith observation of reflection hkl, $\langle I(hkl)\rangle$ is the average intensity of reflection hkl, $\sum_{hkl}$ is the sum over all measured reflections and $\sum_i$ is the sum over i measurements of a reflection.

2.3. Data collection and processing

Crystals were soaked in crystallization buffer containing 25% glycerol or ethylene glycol as a cryoprotectant prior to the X-ray experiment. X-ray diffraction data were collected at 100 K on a MAR 225HE CCD detector installed on BL44XU at SPring-8 (Harima, Japan). The diffraction data were processed with *HKL*-2000 (Otwinowski & Minor, 1997). Molecular replacement (MR) was performed with the *CNS* program package (Brünger *et al.*, 1998; Brunger, 2007).

3. Results

Crystals of PAD3 were obtained within 1–2 weeks at 293 K and diffracted to 2.95 Å resolution. The crystals belonged to space group *R*3, with unit-cell parameters $a = b = 114.97$, $c = 332.49$ Å, $\alpha = \beta = 90$, $\gamma = 120°$, and contained two PAD3 molecules in the asymmetric unit. The calculated $V_{\rm M}$ value was 2.83 Å^3 Da^{-1}, corresponding to a solvent content of 56.6% (Matthews, 1968). Table 1 summarizes the data-collection statistics for the best crystal.

We successfully determined the initial phase by the MR method, using the structure of PAD4 as an initial model. Packing of the MR model showed that two molecules formed a putative dimeric biological unit within an asymmetric unit. The electron density was clearer when noncrystallographic symmetry averaging was used. We are currently engaged in model building and refinement; the detailed molecular structure of PAD3 will be reported in the near future.

We thank Professor Atsushi Nakagawa at the Institute for Protein Research, Osaka University, Japan for his support of our experiments. We also thank the staff members of beamlines BL44XU at SPring-8 and BL17A at Photon Factory (PF) in Japan for data-collection facilities and support. Synchrotron-radiation experiments at SPring-8 and PF were conducted under approval codes 2011B6607 and 2011G518, respectively. This work was supported by Grants-in-Aid for Scientific Research on Innovative Areas (Structural Cell Biology) from the Ministry of Education, Culture, Sports, Science and Technology (MEXT) to MU (23121504).

References

Arita, K., Hashimoto, H., Shimizu, T., Nakashima, K., Yamada, M. & Sato, M. (2004). *Nature Struct. Mol. Biol.* **11**, 777–783.

Arita, K., Hashimoto, H., Shimizu, T., Yamada, M. & Sato, M. (2003). *Acta Cryst.* D**59**, 2332–2333.
Arita, K., Shimizu, T., Hashimoto, H., Hidaka, Y., Yamada, M. & Sato, M. (2006). *Proc. Natl Acad. Sci. USA*, **103**, 5291–5296.
Brunger, A. T. (2007). *Nature Protocols*, **2**, 2728–2733.
Brünger, A. T., Adams, P. D., Clore, G. M., DeLano, W. L., Gros, P., Grosse-Kunstleve, R. W., Jiang, J.-S., Kuszewski, J., Nilges, M., Pannu, N. S., Read, R. J., Rice, L. M., Simonson, T. & Warren, G. L. (1998). *Acta Cryst.* D**54**, 905–921.
Chavanas, S., Méchin, M.-C., Takahara, H., Kawada, A., Nachat, R., Serre, G. & Simon, M. (2004). *Gene*, **330**, 19–27.
Kanno, T., Kawada, A., Yamanouchi, J., Yosida-Noro, C., Yoshiki, A., Shiraiwa, M., Kusakabe, M., Manabe, M., Tezuka, T. & Takahara, H. (2000). *J. Invest. Dermatol.* **115**, 813–823.
Kizawa, K., Takahara, H., Troxler, H., Kleinert, P., Mochida, U. & Heizmann, C. W. (2008). *J. Biol. Chem.* **283**, 5004–5013.
Kizawa, K., Takahara, H., Unno, M. & Heizmann, C. W. (2011). *Biochimie*, **93**, 2038–2047.
Knuckley, B., Causey, C. P., Jones, J. E., Bhatia, M., Dreyton, C. J., Osborne, T. C., Takahara, H. & Thompson, P. R. (2010). *Biochemistry*, **49**, 4852–4863.
Matthews, B. W. (1968). *J. Mol. Biol.* **33**, 491–497.
Méchin, M.-C., Enji, M., Nachat, R., Chavanas, S., Charveron, M., Ishida-Yamamoto, A., Serre, G., Takahara, H. & Simon, M. (2005). *Cell. Mol. Life Sci.* **62**, 1984–1995.
Nachat, R., Méchin, M.-C., Charveron, M., Serre, G., Constans, J. & Simon, M. (2005). *J. Invest. Dermatol.* **125**, 34–41.
Otwinowski, Z. & Minor, W. (1997). *Methods Enzymol.* **276**, 307–326.
Unno, M., Kawasaki, T., Takahara, H., Heizmann, C. W. & Kizawa, K. (2011). *J. Mol. Biol.* **408**, 477–490.
Vossenaar, E. R., Zendman, A. J., van Venrooij, W. J. & Pruijn, G. J. (2003). *Bioessays*, **25**, 1106–1118.
Ying, S., Dong, S., Kawada, A., Kojima, T., Chavanas, S., Méchin, M.-C., Adoue, V., Serre, G., Simon, M. & Takahara, H. (2009). *J. Dermatol. Sci.* **53**, 2–9.